*Materials Science Forum Vols. 595-598 (2008) pp 941-950*
*online at http://www.scientific.net*


# Thermal fatigue of anticorrosive coatings and multilayer coatings: a performance index approach

Pierre D'Ans[1,a], Céline Bondoux[1,b], Christophe Degrandcourt[1], Mohamed Bakrim[2,c], Jean Dille[1,d], Luc Segers[3,e], Marc Degrez[1,f]

[1]Université Libre de Bruxelles (ULB), Crea-Surf team, « Matières et Matériaux » group, 50, Avenue F.D. Roosevelt, CP194/03, 1050 Brussels, Belgium

[2]ALM s.a., Parc Industriel de Fleurus-Farciennes, 25 Lambusart Avenue, 6220 Fleurus, Belgium

[3]Université Libre de Bruxelles (ULB), « Matières et Matériaux » group, 50, Avenue F.D. Roosevelt, CP195/63, 1050 Brussels, Belgium

[a]pdans@ulb.ac.be, [b]cbondoux@ulb.ac.be, [c]mba@almsa.be, [d]jdille@ulb.ac.be, [e]segers@ulb.ac.be, [f]mdegrez@ulb.ac.be

**Keywords:** thermal fatigue, hot metal corrosion, merit factor, performance index, expert system.

**Abstract.** A strategy is proposed to cope with combined thermal fatigue and hot corrosion resistance affecting industrial coatings. It allows comparing different materials, coatings and geometries with respect to thermal cracking and then properly selecting protective coatings. It uses a thermo-mechanical model combining the heat transfer conditions, thermal and mechanical properties of the materials and the system geometry. The model is applied to two cases: (i) borided steel, with experimental support; (ii) multilayer coating made of a thermal barrier layer, aimed at reducing thermal gradients in the system, and a corrosion layer.

## Introduction

To help select and design materials, coatings and surface treatments, databases and expert systems have been regularly investigated in the last 15 years [1-4], with procedures including multi-purpose materials. A companion paper deals with an extension of such expert systems to multi-purpose multi-layer coatings [5], helping to identify the best potential candidates to fulfil given specifications. However, combining certain requirements, like corrosion resistance and thermal fatigue resistance, may prove complex to be incorporated into such expert systems and need an integrated approach. Several surface treatments and coatings were studied recently to protect tools against these aggressive environments, including conversion layers [6-9] and PVD coatings [9-12]. Yet, one lacks a procedure to: (i) predict whether a coating improves or worsens the substrates thermal fatigue resistance; (ii) compare the merits of several single- or multilayer coatings. In fact, the materials submitted to thermal changes face two thermal stresses effects, which add to the deposition stress, in case of coatings [13]:

- *Effect 1*: Thermal stress due to an uneven temperature distribution within the material during transients.

- *Effect 2*: Thermal stress due to unequal thermal expansion coefficient of the materials.

In case of repeated thermal transients, these stresses combine and lead to the so-called thermal fatigue. Effect 1 was successfully modelled for uncoated systems [14-16], taking into account the system geometry, the heat transfer conditions, the thermal expansion and the mechanical properties of the material. Modelling has been done for effect 2 [10, 17]; it was studied in the case of a CrAlN PVD coating submitted to a slow temperature increase (i.e. without effect 1), with the conclusion that the compressive deposition stress counteracts the tensile thermal stress in the coating. However, this finding does not apply to all coatings. Other factors may lower the capacity of these layers to protect the substrate against corrosion [17].

A methodology to compare situations where the geometry, the layers and the substrate are all determining factors in thermal fatigue resistance is presented and illustrated for two practical cases:

(i) *The borided steel thermal fatigue resistance*. Boriding has been proposed by several authors to protect steel from hot metal corrosion [6,7,18], but it sometimes performs poorly when exposed to simultaneous hot metal corrosion and temperature transients [18,19], presumably due to the poor thermal fatigue resistance of the diffusion layer. In this paper, borided steel is experimentally and theoretically studied focussing on changes of number of cycles to failure due to the layer.

(ii) *The thermal fatigue resistance improvement of a material coated against corrosion, using a thermal insulating layer as a top coat* and the discussion of the validity range of such a multilayer.

## Model description

Let us consider an industrial process with temperature changes propagating along x (perpendicular to the surface and the layers), thus assuming a 1D geometry. For slab, cylindrical or spherical geometries, a Matlab® program solves the time dependent heat transfer problem, using the thermal properties of the layers. For instance, the boundary condition can be:

$$k(x)\partial T(x,t)/\partial x = \mp h(t)\left(T_b(t) - T_\infty(t)\right), \quad (1)$$

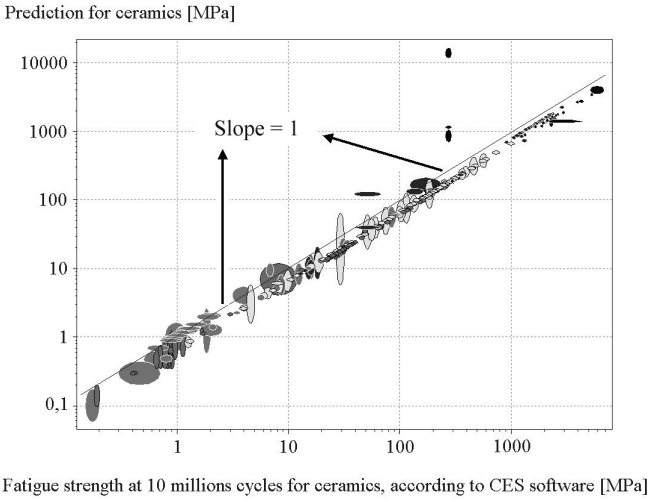


Fig. 1. Eq. (7) validation [1]

where k is the thermal conductivity at each point of the stacking, h is the heat transfer coefficient, $T_b$ is the boundary temperature and $T_\infty$ is the external fluid temperature. $T_\infty$ and h are varied to simulate the different steps of the thermal cycling process. The free thermal deformation of each element of the stacking, $\varepsilon_{th}(x,t) = \alpha(x)\Delta T(x,t)$, is prevented by the mechanical strain of the other elements, $\varepsilon_{average}$. Let $\varepsilon_0$ be the initial deformation of the layer, due to deposition stress. The true mechanical strain of each element to be considered in fatigue constitutive laws is:

$$\varepsilon(x,t)=\varepsilon_0(x)+\varepsilon_{average}(t)-\varepsilon_{th}(x,t). \quad (2)$$

For each cycle, one defines:

$$\Delta\varepsilon(x)=\max(\varepsilon(x))-\min(\varepsilon(x)), \quad (3)$$

$$\bar{\varepsilon}(x)=(\max(\varepsilon(x))+\min(\varepsilon(x)))/2. \quad (4)$$

The latter corresponds to an average stress $\bar{\sigma}$, that takes asymmetric cycles into account. If $\bar{\sigma}=0$, the fatigue resistance is modelled by the Coffin-Manson equation [20]:

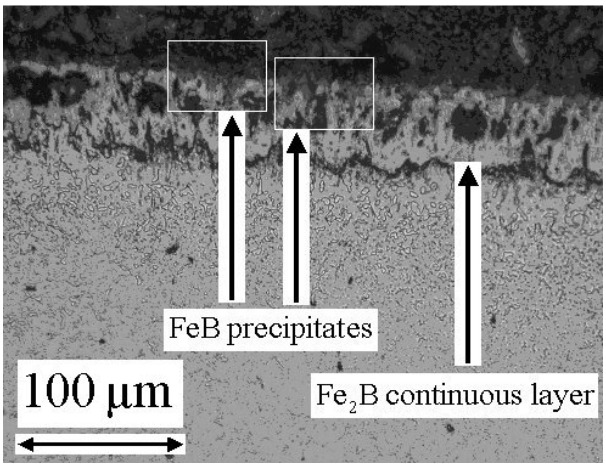


Fig. 2. OM layer cross section.

$$\Delta\varepsilon = M.N_f^z + (G/E)N_f^\gamma, \quad (5)$$

where $N_f$ is the theoretical number of cycles to failure, E is the Young's modulus and $M$, $z$, $G$ and $\gamma$ are experimental parameters. As they are not tabulated, correlations with other mechanical parameters are proposed, like in [21] for ductile materials:

$$\Delta\varepsilon = 3{,}5(\sigma_u/E)N_f^{-0,12} + \varepsilon_u^{0,6}N_f^{-0,6}, \quad (6)$$

where $\sigma_u$ and $\varepsilon_u$ are the ultimate stress and strain. Few results can be found for brittle materials fatigue resistance, excepted in the CES database [1], where the maximum stress amplitude $\Delta\sigma$ at $10^7$ cycles and the ultimate stress can be found. Taking $N_f=10^7$ and $\Delta\sigma=\Delta\varepsilon/E$, one can compare Eq. (6) predictions at $10^7$ cycles with the widely accepted CES data. Taking $N_f=1/4$, the fatigue model should reproduce that $\Delta\sigma\approx 2\sigma_u$. Eq. (6) does not apply to brittle ceramics, for which $\varepsilon_u\approx\sigma_u/E$. In this case, one should use another form of Eq. (5). Knowing the Coffin's correlations for $M$, $z$, $G$ and $\gamma$ (Eq. 4.25 to 4.28 in [20]) and assuming that the reduction of area at rupture is negligible for ceramics and the apparent fracture stress and $\sigma_u$ are nearly equal, one has:

$$\Delta\varepsilon = 2{,}25(\sigma_u/E)N_f^{-0,083}, \quad (7)$$

which better approximates $\Delta\varepsilon=2\varepsilon_u$, when $N_f=1/4$, than Eq. (6). Assuming $N_f=10^7$, a good agreement is found between the prediction of Eq. (7) and CES data (Fig. 1, where each ellipse represents the property range for a tabulated material) [1]. To take the mean stress effect into account, Morrow proposed to replace $\sigma_u$ by $\sigma_u-\bar{\sigma}$ into the Coffin-Manson equation [22]. In a multilayer material with x-dependent properties, Eq. (6-7) become:

$$\Delta\varepsilon_{ductile}(x)=3{,}5((\sigma_u(x)-\bar{\sigma}(x))/E(x))N_f(x)^{-0,12}+\varepsilon_u(x)^{0,6}N_f(x)^{-0,6}, \quad (8)$$

$$\Delta\varepsilon_{brittle}(x)=2{,}25((\sigma_u(x)-\bar{\sigma}(x))/E(x))N_f(x)^{-0,083} \quad (9)$$

Let us solve Eq. (1-4,8,9) for $N_f$ starting with a uniform temperature distribution $T(x,0)=T_0\equiv$ ambient temperature. $T(x)$ at the end of the cycle is no longer uniform and is used as initial condition for the next cycle and similarly for subsequent cycles, which approach a limit cycle. Let successive solutions build a series $N_f(i)$. One stops the iterations at cycle n as soon as

$(N_f(n-1)-N_f(n))/N_f(n)\leq 1\%$. $N_f(n)$ closely approximates the theoretical number of cycles at failure. For each layer, the user chooses between Eq. (8) and (9) for the fatigue description.

**Case study 1: thermal fatigue of borided hot work tool steel**

**Experimental setup.** The substrates consist of H13 hot work tool steel cylinders ($\phi$1cm), in the normalized state, with a hardness of 87 Rockwell B. This thermal treatment was selected to separate the effect of the quenching treatment on the substrate microstructure, from the effect of the layer itself. The substrates were polished using 120 grit SiC paper, degreased with acetone and ethanol and enclosed in a box containing commercial boron carbide pellets (Durferrit Durborid nr3). The box was introduced into the preheated oven and then held 5 hrs at 900°C. The layer cross section was analysed by optical microscopy (OM) after polishing the samples with SiC paper and diamond paste, followed by a nital attack and colorizing with sodium picrate [23]. Nanoindentation measurements with a 8 mN load were performed to evaluate the Young's modulus, according to the method described in [24]. Thermal fatigue testing was then performed using a customized test rig, consisting of an induction coil connected to a Celes generator (24 kW). A piston raises the sample within the coil for heating and lowers it into cold water for cooling. A pyrometer records the superficial temperature of the samples during heating. *Post mortem* sample cross-sections were analysed. Both coated and uncoated samples were tested. Two types of thermal cycles were studied:

- "*Type 1 (T1)*": phase 1: 10 s heating – phase 2: 10 s cooling;
- "*Type 2 (T2)*": phase 1: 5 s heating – phase 2: 10 s cooling.

**Characterization.** OM reveals a 50 µm thick $Fe_2B$ orange-yellow layer, with a typical upper discontinuous pink FeB layer (Fig. 2). Indentation tests were performed along the whole cross section of the layer. The hardness is $16{,}7 \pm 1{,}4$ GPa and the Young's modulus is $336 \pm 25$ GPa.

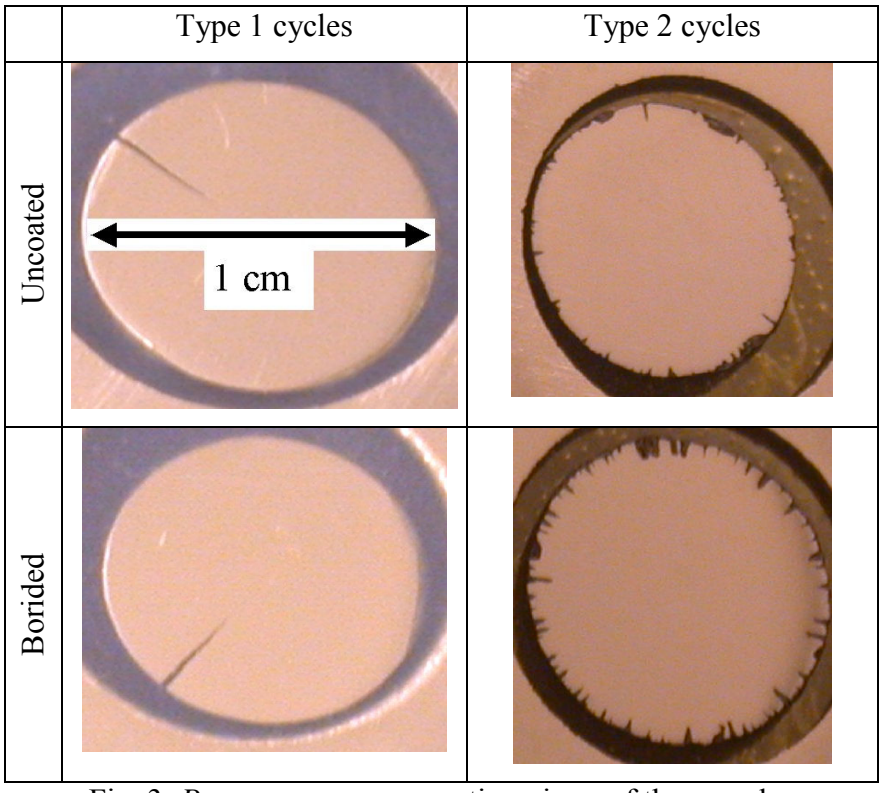

Fig. 3: *Post mortem* cross-section views of the samples

**Thermal fatigue results.** The tests were stopped regularly to check the surface integrity and to evaluate $N_f$ range (sample deformation and cracks propagation). Fig. 3 gives samples *post-mortem* pictures. Table 1 gives the number of cycles at failure. For T1 cycles, deep longitudinal cracks appeared at less than 100 cycles, in both samples. For T2 cycles, the failure occurred sooner on the borided sample than on the uncoated one; after 1000 cycles, the borided sample exhibits denser and deeper cracks. The layer can no longer be observed using OM.

**Strain modelling.** The thermal properties are well documented for $Fe_2B$, making up the layer (table 2). For the boriding layer, $\sigma_0 = \varepsilon_0 E$ is evaluated assuming that the initial stress originates from the thermal expansion mismatch with the substrate and the slow cooling after the process:

$$\sigma_0 \approx E\left(\alpha_{steel} - \alpha_{layer}\right)\left(T_0 - T_{deposition}\right), \qquad (10)$$

In induction heating, the boundary condition is not represented accurately by Eq. (1). The pyrometer temperature record was used as a substitute. Because of boiling during phase 2, Eq. (1) was replaced by [29]:

$$-k\,\partial T/\partial x_b = 2{,}253\left(T_b(t) - T_\infty(t)\right)^{3{,}96}. \qquad (11)$$

The initial temperature is 300 K. Fig. 4 and 5 show strains vs. time for T1 and T2 cycles at different depths: substrate/layer interface and outermost layer surface for coated specimens and at the surface of the uncoated specimens. In both cycles types, the presence of the layer reduces the stress amplitude for steel. The substrate and layer strain amplitude increases when shifting from T2 to T1 cycles.

| Material | Cycle type | Experimental $N_f$ (first cracks) | Calculated $N_f$ | Rank (1 = best resistance) |
|---|---|---|---|---|
| Uncoated H13 | T1 | 30-40 | 206 | 4 |
| Uncoated H13 | T2 | 700-800 | 398 | 1 |
| Coated H13 | T1 | 50-60 | 213 | 3 |
| Coated H13 | T2 | 100-200 | 356 | 2 |

Table.1 Experimental and calculated $N_f$

**Lifetime modelling.** Starting from Fig. 4 and 5 results, $\bar{\varepsilon}$ and $\Delta\varepsilon$ values are used to solve the Eq. (8,9). Steel $\varepsilon_u$ and $\sigma_u$ are taken from literature data [25], but only for the quenched state. $\sigma_u$ is best fit to the observed $N_f$ via the measured hardness (87 Rockwell B), which converts to $\sigma_u = 579$ MPa [31]. Scarce data are available for the layer to set parameters in Eq. (8,9). The difference between the Mann's tensile tests on plain and borided cast stainless steel is rather related to bulk structural changes due to boriding, than to $Fe_2B$ [32]. In [30], bulk $Fe_2B$ stress-strain curves were recorded. If $550°C \le T \le 700°C$: $\sigma_u \approx 300 - 400$MPa, the plastic zone strain varies between 1 and 7 % [30]. In Eq. (8), most parameters are either experimental ($N_f$) or known, excepted $\varepsilon_u$, which varies significantly during the cycle. An equivalent value $\tilde{\varepsilon}_u$ can be fitted to the experimental $N_f$. For instance, using Eq. (8) for ductile materials and taking $\tilde{\varepsilon}_u = 0{,}07$ for the layer, one reproduces a proper ranking of the 4 situations mentioned in Fig. 3 (see table 1).

| | H13 steel | Layer |
|---|---|---|
| $\alpha[°C^{-1}]$ | $13{,}2\,10^{-6}$ [25][a] | $8{,}55\,10^{-6}$ [27][b] |
| $C_p[J/kgK]$ | 608 [25] [a] | 651 [28] |
| $k[W/Km]$ | 30 [25] [a] | 30 [27] |
| $\rho[kg/m^3]$ | 7600 [25] [a] | 7430 [27] |
| $E[GPa]$ | 210 [26] | 336 (see text) |
| $\sigma_0[GPa]$ | 0 | -1,36 (see text) |
| $\varepsilon_u$ | 0,1 [25,26] | 0,01-0,07 |
| $\sigma_u[MPa]$ | 579 (text) | 400 |
| $x[mm]$ | $[0\,;\,4{,}95[$ | $[4{,}95\,;\,5]$ |

Table.2 Relevant properties for modelling

[a] Average value between 25 and 600°C

[b] Average value

The $N_f$ range is in agreement with experimental data (i.e. less than 1000 cycles), but the individuals values are not quantitative.

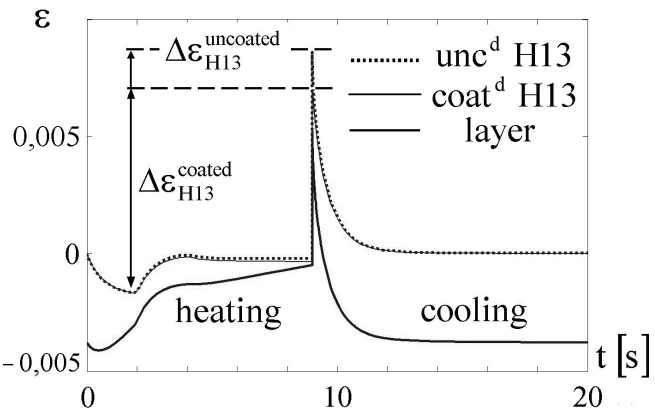


Fig. 4. Strain modelling for T1 cycles

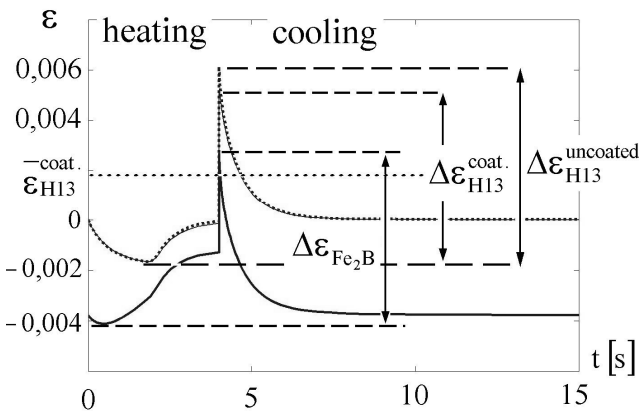


Fig. 5. Strain modelling for T2 cycles

**Discussion.** The model evaluates the strain at each point of a layered material as a function of time during a thermal shock. In the case of a borided steel, it was possible to extract $\Delta\varepsilon$ and $\bar{\varepsilon}$ values, necessary for $N_f$ calculation. $\Delta\varepsilon$ decreases in the underlying steel if it is borided. As in T2 cycles, the layer reduces the overall $N_f$, the superficial mechanical properties are necessarily less favourable than the steel ones. For the layer, $\tilde{\varepsilon}_u$ had to be fitted to experimental $N_f$ values, to reproduce the experimental ranking of the four studied situations. Notwithstanding the fact that the calculated $N_f$ values are within the experimental range, the model under(over)estimates the T1(2) cycles $N_f$, possibly because:

(i) $\tilde{\varepsilon}_u$ does not reflect only the $Fe_2B$ layer intrinsic behaviour, but also the substrate carbide coarsening encountered immediately under the layer, due to the boriding process itself.

(ii) In T1 cycles, the maximum T is higher, so that oxidation is enhanced compared to T2. A complimentary X ray diffraction analysis on debris found in the cooling water shown that they contained iron borates.

(iii) $Fe_2B$ has a low melting point; its properties are expected to be very T-dependent. Besides, the T at which they must be taken in Eq. (8) is not specified.

### Case study 2: study of a multilayer architecture

**Input values.** The studied multilayers are drawn from Srivastava [33], who suggests the following architecture in case of heat checking: low conductivity rare earth oxide/TiAlN chemical barrier layer/Ti bond coat/substrate (where "X/Y" means "X is the top-coat of Y"). In this paper, one considers a semi-infinite vertical slab, horizontally hit at the edge by molten metal (Fig. 6, where y is the distance between a point of the slab and the edge). The multilayer material is made of up to 4 components, whose parameters are given in table 3. The Ti and oxide layers mechanical properties are not taken into account as their properties are not well documented enough. The initial temperature is 373 K. Due to the plane symmetry, $\partial T/\partial x = 0$ at $x = 0$. The other boundary condition is Eq. (1). The cycle is composed of a heating phase (hot fluid penetration, 15 s) and a cooling phase (air, 60 s). To calculate h for the first phase, one uses the following equation,

established for molten metals, for which the thermal and the diffusion boundary layers are not equal [29]:

$$Nu_y := h(y)y/k_{fluid} = 0{,}53\,Pr^{0,5}\,Re_y^{0,5} \text{ with } Pr = \eta C_{P,fluid}/k_{fluid} \text{ and } Re_y = \rho_{fluid} U_\infty y/\eta \quad (12)$$

and where $U_\infty$ is the external fluid velocity (out of the boundary layer), $\eta$ is the viscosity and $C_P$ is the specific heat. Taking a molten medium for which $Pr = 0{,}01353$, $\rho = 2360\,kg/m^3$ and $\eta_{973K} = 0{,}00129\,Pas$ [36-38], one has:

$$h = 8617\sqrt{U_\infty/y}\ [\text{S.I. units}], \quad (13)$$

as long as the Peclet number is comprised between 100 and 10000 [29]: one chooses $y = 0{,}005m$ and $U_\infty = 10\,m/s$ as default values. For the second phase, the process is similar to air quenching, with $h \approx 200\,W/m^2K$ [39].

| | H13 | Ti | TiAlN | Oxide |
|---|---|---|---|---|
| $\alpha[10^{-6}°C^{-1}]$ | 13,2 | 10,1 | 7,48 | 9,05 |
| $C_p[J/kgK]$[c] | 608 | 602 | 792 | 406[d] |
| $k[W/mK]$ | 30 | 22 | 22,5 | 0,69 |
| $\rho[kg/m^3]$ | 7600 | 4500 | 5220[e] | 7650[d] |
| $E[GPa]$ | 140[f] | Not considered | 421[e] | Not considered |
| $\sigma_u[MPa]$ | 800[f] | | 5000[e] | |
| $\varepsilon_u$ | 0,17[f] | | Brittle | |
| $\sigma_0^{293K}[GPa]$ | 0 | | -5 to 0[e] | |
| Thickness | 1 mm[g] | 0,5 µm | 2,5 µm | 1 µm |

Table.3 Materials properties [25,26,33-35]

**Results.** The estimated $N_f$ for the studied situations are reported in table 4 and Fig. 7. The results can be summarized as follows:

(i) The thermal barrier coating improves $N_f$.

(ii) $N_f$ is not sensitive to $\sigma_0$ in TiAlN up to 2,5-3 GPa. For higher values, it drops sharply.

(iii) Exchanging the oxide layer and TiAlN has nearly no effect if $\sigma_0 = -0{,}4GPa$. If $\sigma_0 = -3{,}5GPa$ in the layer, however, the oxide should be in top coat position.

[c] Excepted, mean value between 373 and 973 K

[d] For $CeO_2$

[e] For TiN

[f] At 600°C

[g] Half thickness

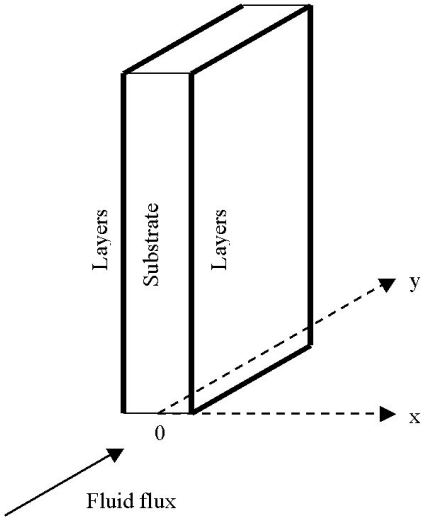


Fig. 6. Problem geometry

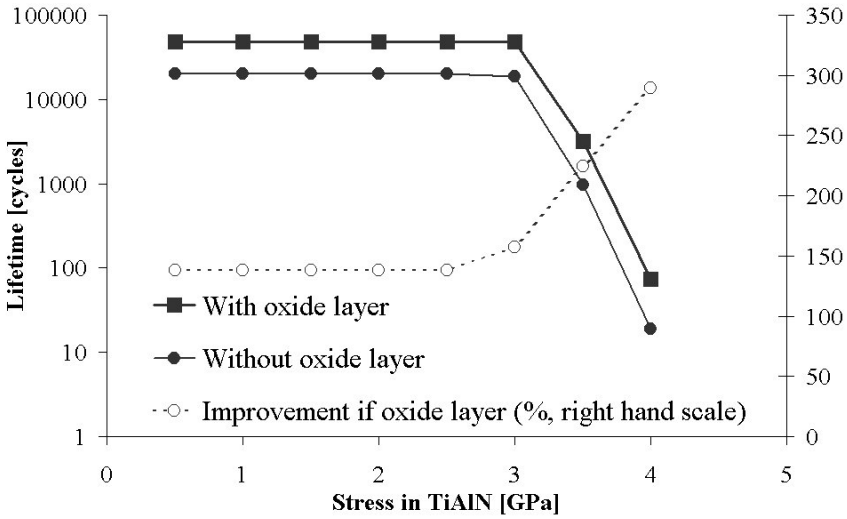


Fig. 7. Effect of the TiAlN deposition stress for oxide/TiAlN/Ti/H13 and TiAlN/Ti/H13.

**Discussion.** In the multilayer, the oxide layer reduces the heat flux, and thus thermal gradients in the underlying stacking, finally increasing $N_f$. In most cases, the steel mechanical properties mostly influence $N_f$, excepted when $\sigma_0$ in the TiAlN exceeds a threshold value; in this case, $N_f$ is very sensitive to $\sigma_0$, which can be tuned by appropriate deposition conditions (i.e. the ionic bombardment intensity or the deposition temperature, for PVD coatings). As long as $\sigma_0$ is not critical, exchanging the thermal barrier and the chemical barrier coatings has no significant effect. Their order can then be chosen based on criteria like a better adherence with the adjacent layers. The relative $N_f$ improvement due to the oxide layer is more significant for higher values of $\sigma_0$ in TiAlN.

| Multilayer | $\sigma_0$[GPa] | $N_f$ |
|---|---|---|
| TiAlN/Ti/H13 | -0,4 | 20 237 |
| Oxide/TiAlN/Ti/H13 | | 48 159 |
| | -3,5 | 3 168 |
| TiAlN/oxide/Ti/H13 | -0,4 | 48 361 |
| | -3,5 | 384 |

Table.4 Results for multilayer coatings

## Conclusions

By evaluating the strain as a function of time at each point of a material, a model allows selecting combinations of substrate, coatings, heat transfer conditions and geometry for the best resistance in thermal fatigue. The model helps explore promising multilayer coatings. It can contribute to tune parameters for coating deposition, if one knows how these influence $\sigma_0$ and to select the thickness of thermal barriers. For more elaborate geometries, one could use FEM with modified Coffin-Manson equations. When a layer parameter, like $\varepsilon_u$, is missing, one can retrieve it by combining the model with experimental results. Such an equivalent value was evaluated in the case of borided steel; it can be reused to study similar configurations. The model is complimentary with the expert system presented in [5], by detecting critical thermal cycling situations and ranking the solutions brought by the software.

**Acknowledgement**

The authors want to acknowledge Prof. Y. Bréchet for a discussion on the content of this paper, the Walloon Region of Belgium and the European Social Funding for the "First Europe" grant.

**References**

[1] *Cambridge selection software, CES* (Granta Design Ltd, Cambridge UK 2000)

[2] Y. Bréchet, D. Bassetti, D. Landru and L. Salvo: Prog. Mater. Sci. Vol. 46 (2001), p. 407

[3] S.E. Franklin and J.A. Dijkman: Wear Vol. 181 (1995), p. 1

[4] A.A. Voevodin, A.L. Erokhin and V.V. Lyubimov: Phys. Stat. Sol. A Vol. 145 (1994), p. 565

[5] C. Bondoux, C. Degrandcourt, G. Ailinca, P. D'Ans, M. Degrez, D. Wathelet, F. Barthélémy, J. Anciaux, G. Ospina and J.M. Jacquet: *this congress*

[6] D. N. Tsipas, G. K. Triantafyllidis, J. Kipkemoi Kiplagat and P. Psillaki: Mater. Lett. Vol. 37 (1998), p. 128

[7] D.C. Lou, O.M. Akselsen, M.I. Onsøien, J.K. Solberg and J. Berget: Surf. Coat. Technol. Vol. 200 (2006), p.5282

[8] V. Joshi, A. Srivastava, R. Shivpuri and E. Rolinski: Surf. Coat. Technol. Vol. 163-164 (2003), p. 668

[9] V. Joshi, K. Kulkarni, R. Shivpuri, R. S. Bhattacharya, S. J. Dikshit and D. Bhat: Surf. Coat. Technol. Vol. 146-147 (2001) p. 338

[10] M. Pellizzari, A. Molinari and G. Straffelini: Surf. Coat. Technol. Vol. 142-144 (2001), p. 1109

[11] C. Mitterer, F. Holler, F. Üstel and D. Heim: Surf. Coat. Technol. Vol. 125 (2000), p. 233

[12] Y. Wang: Surf. Coat. Technol. Vol. 94-95 (1997), p. 60

[13] R. Ebner, S. Marsoner, I. Siller and W. Eker in: Proc. of *Tool06*, edited by AIM, Italy (2006)

[14] A. Persson, S. Hogmark and J. Bergström: J. Mat. Proc. Tech. Vol. 152 (2004), p. 228

[15] A. Srivastava, V. Joshi and R. Shivpuri: Wear Vol. 256 (2004), p. 38

[16] F. Medjedoub, G. Dour and F. Rézaï-Aria: Fonderie Fondeur d'Aujourd'hui Vol.244 (2005), p. 22.

[17] P. D'Ans, M. Bakrim, M. Brizuela, A. García-Luis, L. Segers and M. Degrez in: Proc. of *Matériaux 2006*, edited by FFM, France (2006)

[18] P. Hairy and R. Dussaussois: Fonderie Fondeur d'Aujourd'hui Vol. 227 (2003), p. 30

[19] A. Persson, S. Hogmark and J. Bergström: Surf. Coat. Technol. Vol. 191 (2005), p. 216

[20] S. S. Manson: *Thermal Stress and Low-cycle Fatigue* (McGraw-Hill, USA 1966)

[21] G. E. Dieter: *Mechanical Metallurgy* (MacGraw-Hill, USA 1983)

[22] J. Morrow: ASTM STP Vol. 378 (1965), p. 45-87

[23] S. Ramain: *PhD thesis* (University of Perpignan, France 1983)

[24] W. C. Oliver and G. M. Pharr: J. Mat. Res. Vol. 7 (1992), p. 1564

[25] *Orvar® Supreme, Hot Work Tool Steel*, technical note, Uddeholm

[26] MatWeb database (www.matweb.com)

[27] H.J. Hunger: *Boronizing to produce wear-resistant surface layers* (Bortec GMBH)

[28] I. Barin: *Thermochemical properties of inorganic substances* (Springer-V., Germany 1977)

[29] J. P. Holman: *Heat Transfer* (McGraw-Hill, USA 1989)

[30] H. Taga and H. Yoshida: Met. Sci. Vol. 8 (1974), p. 222

[31] Hardness conversion table (http://www.gordonengland.co.uk)

[32] B.S. Mann: Wear Vol. 208 (1997), p.125

[33] A. Srivastava, V. Joshi, R. Shivpuri, R. Bhattacharya and S. Dixit: Surf. Coat. Technol. Vol. 163 (2003), p. 631

[34] O. Kubaschewski: *Metallurgical thermochemistry* (Pergamon, UK 1967)

[35] V. Ji: *habilitation à diriger des recherches* (UST Lille, France 2003)

[36] R.N. Singh, S. Arafin and A.K. George: Physica B Vol.387 (2007), p. 344

[37] C.J. Smithells: *Metals Reference Book* (Butterworths, UK 1976)

[38] A.T. Dinsdale and P.N. Quested: J. Mat. Sci. Vol. 39 (2004), p. 7221

[39] *ASM Handbook* Vol. 4, p. 72 (ASM International, USA 1991)